# Steady grey solitary capillary-gravity waves on a conducting fluid under effects of vertical electric fields

April 6, 2017

**Abstract**

In the present work, we aim to compute fully nonlinear steady and time-dependent solutions of the electrohydrodynamic problem (EHD) with the help of a conformal mapping technique. Bifurcations of travelling waves are considered. A branch of grey solitary waves is found to be connecting two branches of Stokes waves.

## 1 Introduction

Electrohydrodyanmics (EHD) is a topic which is concerned with the dynamics of electrified fluids. In particular, the problem of waves on an electrified interface (between liquid and air or two dielectric fluids with different permittivities) attracts much research attention because of its vast industrial applications such as coating processes, cooling systems, electrowetting and etc. (see [1] and references therein). It was previously pioneered by a few works in the 60s (see [13] for a review). A descent understanding of EHD mechanism is helpful in advancing and innovating the industrial applications.

Tangential (horizontal) electric fields have effect of stabilising the interface due to its dispersive contribution in the linear regime, e.g. suppressing Rayleigh-Taylor instability, retarding the film rupture as shown in [2, 22]. Capillary waves on a fluid sheet under the effects of tangential electric fields were considered in [19, 17]. A boundary integral equation method was used to compute fully nonlinear solutions. Also weakly nonlinear solutions were studied analytically by assuming the long wave approximation limit. On contrast, normal (vertical) electric fields have effect of destabilising the interface. The problem was investigated in [9, 18, 20] where an asymptotic model equation for long waves was derived and fully nonlinear solutions were again computed by a boundary integral method. More recently, model equations were derived in [26] for the problem where the fluid in the lower tier is assumed to be perfectly conducting for long waves and short waves in addition to [11] where a Benjamin-Ono Kadomtsev-Petviashvili model was derived. For the same problem, the local bifurcation of solitary waves was investigated in [12] by using a quintic model equation. In the present work, we aim to study the interface between a conducting fluid and air under vertical electric fields. By [10], the linear dispersion

relation for this problem is written as

$$c_p^2 = \frac{g}{k} - \frac{\epsilon_0 V_0^2}{\rho} + \frac{\sigma}{\rho}k, \tag{1}$$

where $c_p$ is the phase speed, $k$ is the wavenumber, $g$ is the gravity, $V_0$ is the strength of the electric field at infinity, $\epsilon_0$ is the permittivity of the air, $\rho$ is the density of the fluid and $\sigma$ is the surface tension. Following [12, 26], the associated Nonlinear Schrödinger Equation (NLS) changes type at certain values of the electric parameter. It worth having a recap on two classical water wave problems associated with different types of NLS in the next paragraph.

When the electric fields are absent, it reduces to the classical capillary-gravity (CG) problem which has been studied intensively during the last a few decades. Under deep water regime, the linear dispersion relation reads

$$c_p^2 = \frac{g}{k} + \frac{\sigma}{\rho}k. \tag{2}$$

$c_p$ attains a minimal value when $k = \sqrt{\rho g/T}$. The associated NLS is of focussing type, which predicts the existence of bright solitary waves. They bifurcate at the speed minimum from infinitesimal periodic waves and travel with a speed which also equals the group speed $c_g$. For a full review on the capillary-gravity problem, the readers are referred to [4, 3, 16, 23] and references therein. A related topic but with a different type of NLS is the so-called flexural-gravity (FG) problem which enjoys a direct application in the waves deformed beneath ice sheets. The linear dispersion relation is

$$c_p^2 = \frac{g}{k} + \frac{D}{\rho}k^3, \tag{3}$$

which admits a minimum at $k = \sqrt[4]{\rho g/3D}$. $D$ is the flexural rigidity. Its associated NLS is defocussing and therefore only predicts the existence of dark solitary waves as were found in [15] where Kirchhoff-Love (KL) model [5, 6] was used for the pressure exerted by the elastic sheet above the fluid. However bright solitary waves with finite amplitude, although not predicted by the NLS, could still exist and bifurcate at the speed minimum and were found in [14] and in [7] by employing KL and Plotnikov-Toland model [21] respectively. These two non-electric problems with different associated NLS provide insights on how the solutions behave at small amplitudes. In this paper, we consider two-dimensional progressive waves propagating on the surface of a conducting fluid in the presence of vertical electric fields. The associated NLS changes type at some certain values of the electric-related parameter by [26]. In this work we are particularly interested in the case where the NLS is defocussing. The bifurcation structure of solitary waves for this EHD problem is investigated and compared to ones of CG and FG.

The paper is organised as follows. In section 2, we provide the detailed formulation for the problem. It follows by stating the conformal mapping technique and the numerical method in section 3. The computational results are presented in section 4. The conclusions are given in section 5.

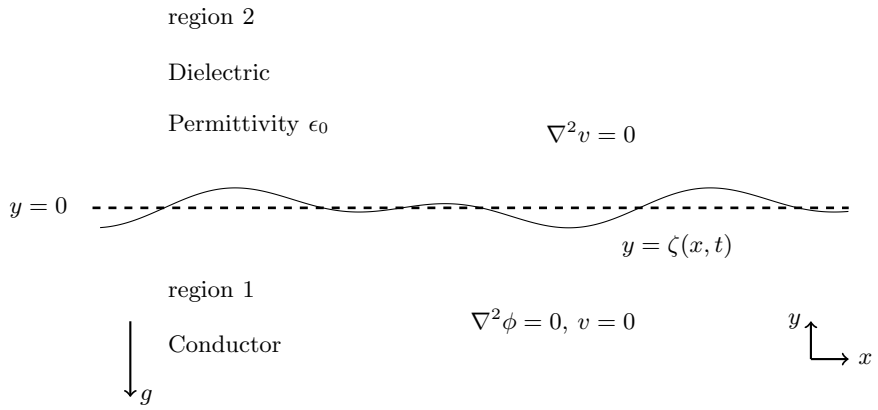


Figure 1: Configuration of the problem. The gravity acts in the negative $y$-direction. We denote the equation of the unknown free surface by $y = \zeta(x,t)$.

## 2 Formulation

We consider a two-dimensional irrotational flow of an incompressible, inviscid and perfectly conducting fluid with infinite depth (region 1). In the region above (region 2), the air is assumed to be hydrodynamically passive with permittivity $\epsilon_0$. The problem can be formulated by using Cartesian coordinates with the $y$-axis directed vertically upwards and $y = 0$ at the undisturbed level. The gravity $g$ and the surface tension $\sigma$ are both included in the formulation. The deformation of the free surface is denoted by $\zeta(x,t)$. A vertical electric field with voltage potential $v$ is applied. We assume that $v \sim V_0 y$ as $y \to \infty$, where $V_0$ is a constant. Since the fluid motion can be described by a velocity potential function $\phi(x,y,t)$, introducing dimensionless variables by choosing

$$\left(\frac{\sigma}{\rho g}\right)^{\frac{1}{2}}, \quad \left(\frac{\sigma}{\rho g^3}\right)^{\frac{1}{4}}, \quad V_0 \tag{4}$$

as the reference length, time and voltage potential, the governing equations can then be written as

$$\Delta\phi = 0, \qquad \text{for} \quad y < \zeta(x,t), \tag{5}$$
$$\Delta v = 0, \qquad \text{for} \quad y > \zeta(x,t), \tag{6}$$
$$\zeta_t = \phi_y - \phi_x\zeta_x, \qquad \text{on} \quad y = \zeta(x,t), \tag{7}$$
$$v = 0, \qquad \text{on} \quad y \le \zeta(x,t), \tag{8}$$
$$v_y \sim 1, \qquad \text{as} \quad y \to \infty, \tag{9}$$
$$\phi_y \to 0, \qquad \text{as} \quad y \to -\infty. \tag{10}$$

and

$$\phi_t = -\frac{1}{2}|\nabla\phi|^2 - y - \frac{\beta}{1+\zeta_x^2}\Big[\frac{1}{2}(1-\zeta_x^2)(v_x^2 - v_y^2) + 2\zeta_x v_x v_y\Big] + \frac{\zeta_{xx}}{(1+\zeta_x^2)^{3/2}} - \mathcal{P}_e + B, \quad \text{on} \quad y = \zeta(x,t), \tag{11}$$

where the subscripts denote the partial derivatives, $\Delta = \partial_x^2 + \partial_y^2$ defines the Laplacian and

$$\beta = \epsilon_0 V_0^2 \sqrt{\frac{\rho g}{\sigma^3}} \tag{12}$$

is a parameter which measures the ratio of electric and gravitational force to surface tension. $\mathcal{P}_e$ describes the external forcing. $B$ is the Bernoulli constant. By using (8) in the dynamic boundary condition, (11) is simplified as

$$\phi_t = -\frac{1}{2}|\nabla\phi|^2 - y + \frac{\beta}{2}|\nabla v|^2 + \frac{\zeta_{xx}}{(1+\zeta_x^2)^{3/2}} - \mathcal{P}_e + B, \quad \text{on} \quad y = \zeta(x,t). \tag{13}$$

Following [12], after performing the normal form analysis by introducing $X = \epsilon x$ and $T = \epsilon^2 t$, we retrieve the dispersion relation at the linear order

$$\omega^2 = k + k^3 - \beta k^2 \quad \text{or} \quad c_p^2 = \frac{1}{k} + k - \beta, \tag{14}$$

where $k$ is the wavenumber and $\omega$ is the frequency. Here we also assumed that the wave travels in the positive direction, i.e. rightwards. At the next order we obtain the group speed

$$c_g = \frac{1 + 3k^2 - 2\beta k}{2\omega}. \tag{15}$$

At the cubic order, we have the Nonlinear Schrödinger Equation

$$iA_T + \frac{3k - c_g^2 - \beta}{2\omega} A_{XX} + \alpha |A|^2 A = 0 \tag{16}$$

where

$$\alpha = \frac{k}{2\omega}\Big[\frac{2(\beta k^2 - \omega^2)^2}{2k^2 - 1} - 2k^2 - \frac{k^4}{2}\Big]. \tag{17}$$

At $k = 1$, the phase speed $c_p$ attains its minimum $c^* = \sqrt{2-\beta}$ and equals the group speed $c_g$ where the solitary waves may bifurcate from infinitesimal periodic waves provided that the corresponding NLS is of focussing type. The NLS reads

$$iA_T + \lambda A_{XX} + \gamma |A|^2 A = 0 \tag{18}$$

where

$$\lambda = \frac{1}{2\sqrt{2-\beta}}, \qquad \gamma = \frac{4}{\sqrt{2-\beta}}\Big[(\beta-1)^2 - \frac{5}{16}\Big]. \tag{19}$$

Thus the NLS is of focussing type if

$$0 < \beta < 1 - \frac{\sqrt{5}}{4} \simeq 0.441 \quad \text{or} \quad 1.559 \simeq 1 + \frac{\sqrt{5}}{4} < \beta < 2. \tag{20}$$

The coefficient of the nonlinear term in (19) changes sign at two critical values $1 \pm \frac{\sqrt{5}}{4}$. In this paper, we restrict our attention to the case where $\beta = 0.5$ such that the associated NLS is of defocussing type.

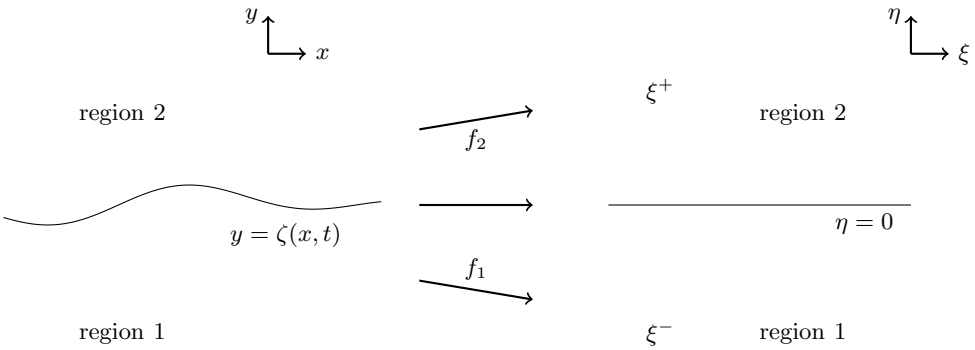


Figure 2: Schematic of the conformal mapping.

# 3 Conformal mapping and numerical scheme

We introduce two time-dependent conformal mappings, $f_1$ and $f_2$, which map the fluid domain $y < \zeta(x,t)$ and above region $y > \zeta(x,t)$ onto the lower half and the upper half $(\xi, \eta)$-plane respectively. $\xi$ in the upper layer is denoted by $\xi^+$ and in the lower layer by $\xi^+$. In the mapped plane, we defined spatial variables on the surface as $X^\pm = X(\xi^\pm, t) \equiv x(\xi^\pm, 0, t)$, $Y^\pm = Y(\xi^\pm, t) \equiv y(\xi^\pm, 0, t)$. $f_1$ can be found by solving the boundary value problem

$$\Delta^- y = 0, \qquad \eta < 0, \tag{21}$$
$$y = Y(\xi^-, t), \qquad \eta = 0, \tag{22}$$
$$y \sim \eta, \qquad \eta \to -\infty, \tag{23}$$

and similarly for $f_2$, we need to solve

$$\Delta^+ y = 0, \qquad \eta > 0, \tag{24}$$
$$y = Y(\xi^+, t), \qquad \eta = 0, \tag{25}$$
$$y \sim \eta, \qquad \eta \to \infty, \tag{26}$$

where $\Delta^\pm = \partial^2_{\xi^\pm} + \partial^2_\eta$. After some algebra, we obtain two relations on the surface

$$X^- = \xi^- - \mathcal{H}[Y^-], \tag{27}$$
$$X^+ = \xi^+ + \mathcal{H}[Y^+], \tag{28}$$

where $\mathcal{H}[.]$ is the Hilbert transform which can be defined as

$$\mathcal{H}[g](\xi) = \mathrm{PV} \int_{-\infty}^{\infty} \frac{g(\xi')}{\xi' - \xi} d\xi'. \tag{29}$$

Then we introduce the harmonic conjugates of $\phi(\xi^-, \eta)$ and $v(\xi^+, \eta)$, denoted by $\psi(\xi^-, \eta)$ and $w(\xi^+, \eta)$ respectively. On the surface we define $\Phi(\xi^-, t) \equiv \phi(\xi^-, 0, t)$, $\Psi(\xi^-, t) \equiv \psi(\xi^-, 0, t)$, $V(\xi^+, t) \equiv v(\xi^+, 0, t)$ and $W(\xi^+, t) \equiv w(\xi^+, 0, t)$.

To ease the notations, we use $\xi$ in the place of $\xi^-$ hereafter. By solving the Laplace problem in region I for t$\phi$ and in region II for the $v$, we get

$$\Psi_\xi = \mathcal{H}[\Phi_\xi], \tag{30}$$

$$W_{\xi^+} = -1 - \mathcal{H}[V_{\xi^+}]. \tag{31}$$

We note that $V_{\xi^+}$ is constantly zero due to condition (8). In particular for travelling waves with a speed $c$, after some similar calculations as shown in [16], we obtain the governing equation for steady solutions

$$\frac{c^2}{2}\Big(\frac{1}{J}-1\Big) + Y - \frac{X_\xi Y_{\xi\xi} - Y_\xi X_{\xi\xi}}{J^{3/2}} - \frac{\beta}{2}\Big(\frac{1}{J^+}-1\Big) + \mathcal{P}_e = B. \tag{32}$$

with $J^+ \equiv X^2_{\xi^+} + Y^2_{\xi^+}$ and $J \equiv X^2_\xi + Y^2_\xi$. All the terms in (32) are evaluated at $\xi$ except $-\frac{\beta}{2}\frac{1}{J^+}$, which is the contribution by the electric fields, needs to be evaluated at $\xi^+$.

In order to compute fully localised nonlinear solutions, we approximate the solitary waves by long periodic waves with wavelength $L$. The surface elevation can be expressed by using Fourier series,

$$Y(\xi,t) = \sum_{n=1}^{N} a_n \cos(\frac{2n\pi\xi}{L}) + \sum_{n=1}^{N} b_n \sin(\frac{2n\pi\xi}{L}), \tag{33}$$

where the Fourier coefficients $a_n$ and $b_n$ are all time-dependent and the series is truncated after $N$ terms. In particular for waves which are symmetric by $\xi = 0$, all the $b_n$ are zero. $L$ is chosen sufficiently large so that the results hardly change as $L$ is further increased. In most calculations, we use $L = 39\pi$. The Hilbert transform can be numerically computed by

$$\mathcal{H}[g] = \mathcal{F}^{-1}(isgn(k)\mathcal{F}[g]), \tag{34}$$

where $\mathcal{F}$ is the Fourier transform. We introduce $2N$ collocation points uniformly distributed along $\xi$ in $[-L/2, L/2)$ from the lower side of the surface in the mapped plane. In the physical plane, we require

$$X^+ = X^-, \tag{35}$$

$$Y^+ = Y^-, \tag{36}$$

to match the points $\xi^+$ from the upper side and $\xi$ from the lower side. Then $\xi^+$ can be written in terms of $\xi$ by using (27) and (28). All the non-electric terms are computed directly on $\xi$. To compute the electric contribution in the dynamics boundary condition, we need to find the value of $J^+$. This can be achieved by using chain rule and trigonometric interpolations on $J$. The dynamic boundary condition is satisfied on the collocation points, which provide $2N$ algebraic equations. The Fourier coefficients are the unknowns which are solved numerically via Newton's method. The wave amplitude is defined by

$$A = \frac{1}{2}\Big(\max(y) - \min(y)\Big), \tag{37}$$

which is used as a parameter. The Bernoulli constant $B$ is an unknown which is uniquely determined by setting the mean level of surface elevation to be zero.

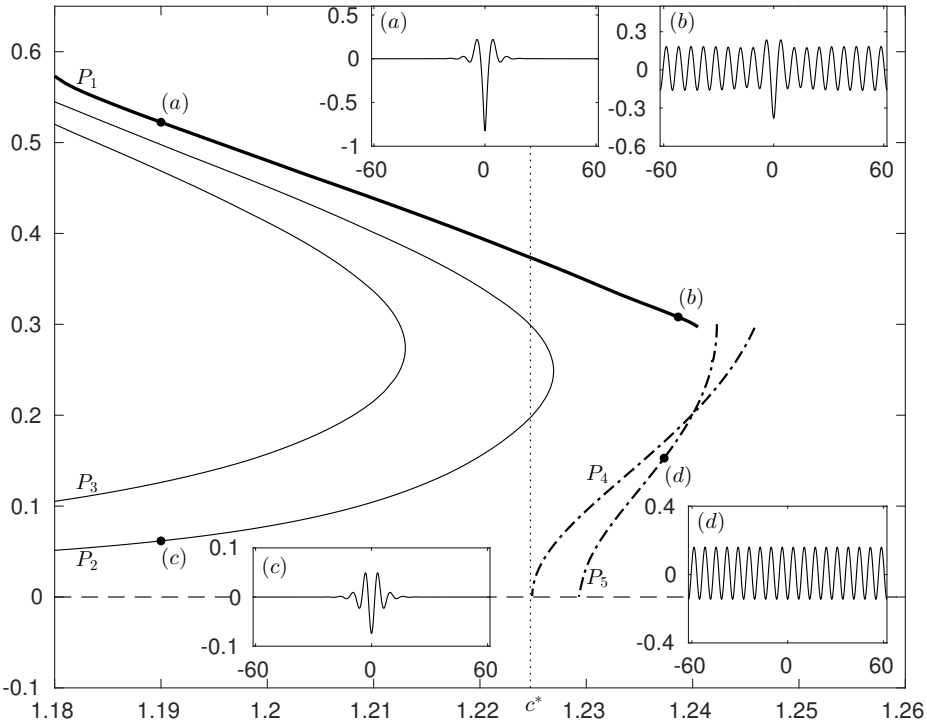


Figure 3: Amplitude-speed bifurcation diagram. $P_1$ is the branch of free depression solitary waves. $P_2$ and $P_3$ are the branches of forced depression solitary waves. $P_4$ and $P_5$ are two branches of periodic Stokes waves. Typical wave profiles are presented in the physical plane.

# 4 Results

We start with computing bright depression solitary waves (BDS), whose amplitude is zero in the far field and non-zero in the middle, by introducing the external forcing $\mathcal{P}_e$ which is defined as

$$\mathcal{P}_e(\xi) = a\cos\xi\exp(-\frac{\xi^2}{16}), \tag{38}$$

for different values of $a$. Two branches of forced solitary depression waves are shown in figure 3 as $P_2$ for a smaller forcing with $a = 0.02$ and $P_3$ for a larger forcing with $a = 0.05$. By removing $\mathcal{P}_e$, a branch of free solitary waves is obtained and denoted by $P_1$. The free depression solitary waves of $P_1$ bifurcate at the minimum phase speed $c^* = \sqrt{1.5}$ with finite amplitude. No solitary waves bifurcate can from infinitesimal periodic waves as predicted by the NLS. By following the branch $P_1$ beyond $c^*$, ripples of constant amplitude are observed in the far field due to a resonance with periodic waves with the same speed. These waves with non-decaying tails are the so-called generalised solitary waves(GSW) (see ($b$) in figure 3). Tracking further on $P_1$, the amplitude of ripples in the far field becomes larger and the difference between the central trough and the other troughs gets smaller. As a consequence, $P_1$ eventually joins a branch of

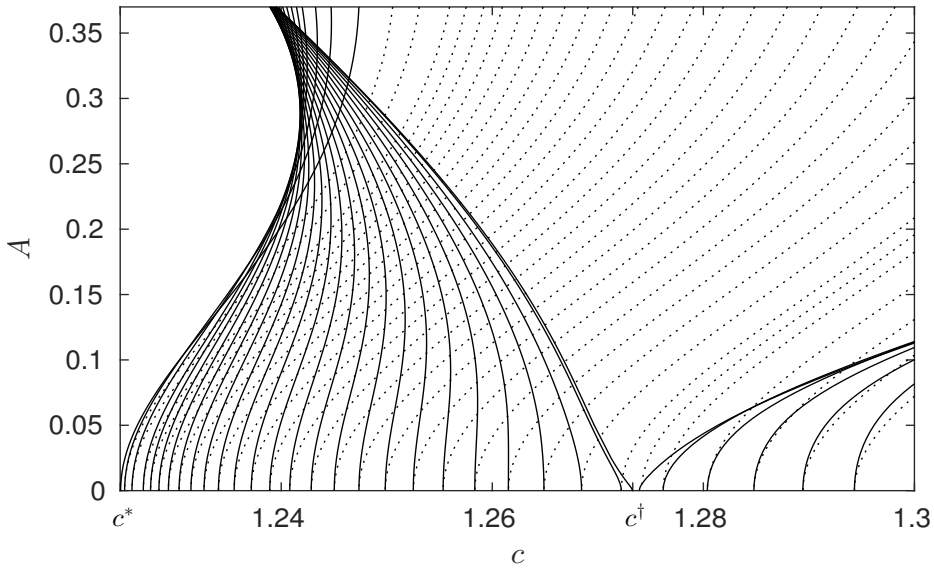


Figure 4: Branches of Stokes waves. The solid curves are the branches of shorter waves with $k < k^* = 1$ whereas the dotted curves are for longer waves with $k > k^* = 1$. The very left branch corresponds to $k = k^*$, i.e. $2\pi$ periodicity.

periodic Stokes waves (SW) as the gap between the troughs shrinks to zero. Linear periodic waves bifurcate at zero amplitude with different phase speed for different wavenumber. The lowest possible speed occurs when the wavenumber $k = k^* = 1$, i.e. with $2\pi$ periodicity. This branch is denoted by $P_4$ in figure 3. The hydroelastic problem, where the associated NLS is also of defocussing type, was studied in [14] by using the Full Euler equations based on the same formulation as introduced in section 2 and 3. They found a similar bifurcation diagram of depression solitary waves. More recently the local bifurcation of this problem was studied by using a quintic model equation in [12], where the results agreed well with ours.

The NLS predicts the existence of dark solitary waves (DS) which bifurcate at the minimum speed $c^*$ with zero amplitude. These solutions have oscillating tails in the far field and decay to zero at the axis of symmetry in the middle. They were computed in [15] for the hydroelastic problem and in [12] for the EHD problem. Grey solitary waves (GS), a generalised version of dark solitary waves, are similarly defined except the amplitude of the central crest of trough is non-zero and smaller than those at the tails. They can be also treated as a continuation of generalised solitary waves whose central crest or trough is larger than the others in the far field. To better under the origin of GS, it worth carrying out a complete investigation on the bifurcation of periodic waves. The results are presented in figure 4 for various values of $k$ near $k^* = 1$. The wave with $2\pi$ periodicity has the lowest speed at small amplitudes. Shorter Stokes waves with $k > k^*$ are monotonic in $c$ as $A$ is increased. They are sketched as the dotted curves in figure 4. However longer Stokes waves with $k < k^*$ reach a minimum speed at finite amplitudes. The branches meet almost at a

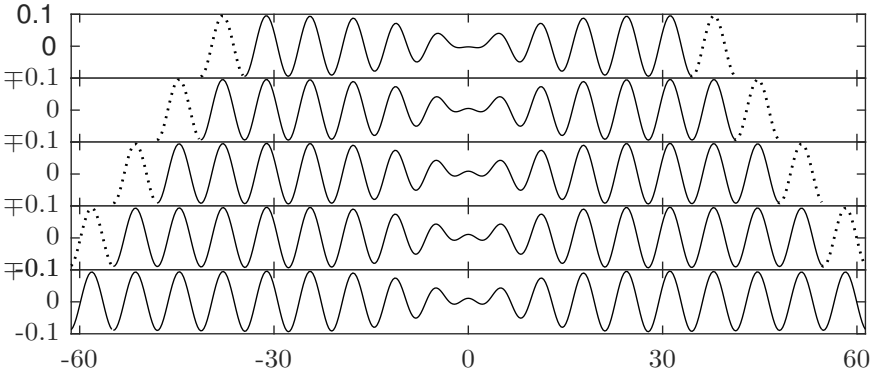


Figure 5: Construction of grey solitary waves. The wave profiles are sketched in the physical plane.

fold point where the lowest speed wave occurs on the branch corresponding, at small amplitude, to 'Wilton' ripples. A Stokes expansion is required to find the wavenumber at which 'Wilton' ripples bifurcate and the answer is found to be

$$k^\dagger = \frac{1}{\sqrt{2}} \quad \text{or} \quad c^\dagger = \sqrt{\frac{3\sqrt{2}-1}{2}} \simeq 1.2733. \tag{39}$$

The readers are referred to [23] for more details on 'Wilton' ripples.

In order to find GS, we start with computing Stokes waves with $L = 22\pi$ and $k = k^* = 1$, i.e. 11 peaks in the domain. By using the same mechanism as described in [8], we follow this solution branch and monitor the value of the associated Jacobian which changes sign if a bifurcation takes place. We manage to locate a bifurcation point at which a new solution branch emanates. A typical wave profile is displayed on top in figure 5. This periodic solution already looks like a truncated grey solitary wave. Being inspired by the work in [24], we add an extra ripple at each end of the wave to form an initial guess for Newton's solver. The value of $A$ is fixed during these computations. It is illustrated in figure 5 with the solid curves representing the convergent solutions which form the initial guesses together with the dotted curves (the extra ripples). By continuing this numerical approach, a wave with infinitely many ripples of constant amplitude in the far field can be obtained, i.e. the grey solitary wave. We work numerically on a truncated grey soliton solution, i.e. with finite wavelength, that does change as more ripples are added in the far field. Under this criterion, the solution on the bottom of figure 6 is selected. By using the continuation method, a complete bifurcation diagram is computed and shown in figure 6. The branch of grey solitary waves, denoted by $P_8$, connects two branches of Stokes waves, denoted by $P_6$ and $P_7$ respectively, where the solution from $P_6$ has one more peak than that from $P_7$ within the same length $L = 39\pi$. In particular, solution $(b)$ has a zero $y$-intercept, i.e. a dark solitary wave. Unlike [12, 15] where external forcing is employed, we manage to find the DS by using an alternative approach.

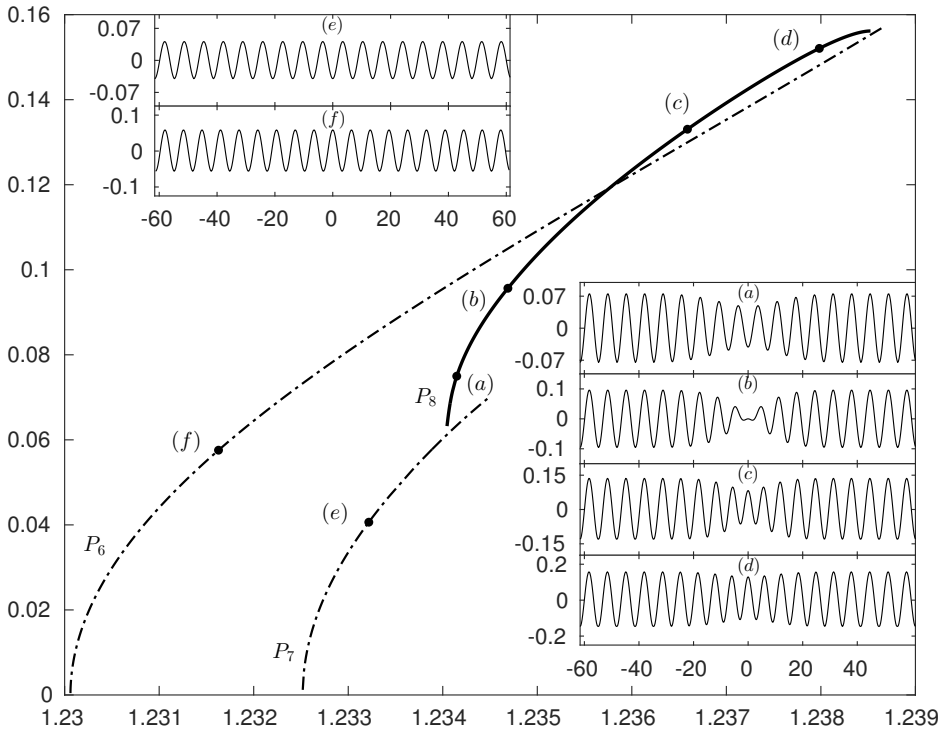


Figure 6: Amplitude-speed bifurcation diagram of grey solitary waves. $P_8$: Branch of grey solitary waves (solid). $P_6$ and $P_7$: Branches of Stokes waves (dotted-dashed). Typical wave profiles are presented in the physical plane..

# 5 Conclusion

In this work, the problem of steady solitary waves on the surface of a conducting fluid with the presence of vertical electric fields was studied. We introduced a valid numerical method, where interpolation was used to match the collocation points on the interface to compute for steady and time-dependent solutions. Our attention was restricted when the electric parameter $\beta = 0.5$ where the associated NLS is defocussing. The complete bifurcation diagrams of bright depression solitary waves, Stokes waves and grey solitary waves were presented. The stability of depression waves was examined numerically. An experiment of head-on collision was performed. Overall these electrified steady solutions had capillary-gravity-like wave profiles but with flexural-gravity-like bifurcation structures. For computing grey solitary waves, we used a similar method as described in [24]. This approach suggests the possibility of computing grey solitary wave solutions with the absence of electric fields and surface tension, i.e. pure gravity waves, which are going to be new families in addition to the ones in [25].

# References


[1] Chen, X., Cheng, J., Yin, X.: Advances and applications of electrohydrodynamics. Chinese Science Bulletin **48**(11), 1055–1063 (2003)

[2] Cimpeanu, R., Papageorgiou, D.T., Petropoulos, P.G.: On the control and suppression of the Rayleigh-Taylor instability using electric fields. Physics of Fluids **26**(2), 022,105 (2014)

[3] Dias, F., Kharif, C.: Nonlinear gravity and capillary-gravity waves. Annual review of fluid mechanics **31**(1), 301–346 (1999)

[4] Dias, F., Menasce, D., Vanden-Broeck, J.-M.: Numerical study of capillary-gravity solitary waves. European journal of mechanics. B, Fluids **15**(1), 17–36 (1996)

[5] Forbes, L.K.: Surface waves of large amplitude beneath an elastic sheet. part 1. high-order series solution. Journal of Fluid Mechanics **169**, 409–428 (1986)

[6] Forbes, L.K.: Surface waves of large amplitude beneath an elastic sheet. part 2. Galerkin solution. J. Fluid Mech **188**(1), 491–508 (1988)

[7] Gao, T., Wang, Z., Vanden-Broeck, J.-M.: New hydroelastic solitary waves in deep water and their dynamics. Journal of Fluid Mechanics **788**, 469–491 (2016)

[8] Gao, T., Wang, Z., Vanden-Broeck, J.-M.: Investigation of symmetry breaking in periodic gravity–capillary waves. Journal of Fluid Mechanics **811**, 622–641 (2017)

[9] Gleeson, H., Hammerton, P., Papageorgiou, D., Vanden-Broeck, J.-M.: A new application of the Korteweg–de Vries Benjamin-Ono equation in interfacial electrohydrodynamics. Physics of Fluids (1994-present) **19**(3), 031,703 (2007)

[10] Hunt, M.: Linear and nonlinear free surface flows in electrohydrodynamics. Ph.D. thesis, University College London (2013)

[11] Hunt, M., Vanden-Broeck, J.-M., Papageorgiou, D., Parau, E.: Benjamin-Ono Kadomtsev-Petviashvili's models in interfacial electro-hydrodynamics. European Journal of Mechanics-B/Fluids (2017)

[12] Lin, Z., Zhu, Y., Wang, Z.: Local bifurcation of electrohydrodynamic waves on a conducting fluid. Physics of Fluids **29**(3), 032107 (2017)

[13] Melcher, J., Taylor, G.: Electrohydrodynamics: a review of the role of interfacial shear stresses. Annual review of fluid mechanics **1**(1), 111–146 (1969)

[14] Milewski, P.A., Vanden-Broeck, J.-M., Wang, Z.: Hydroelastic solitary waves in deep water. Journal of Fluid Mechanics **679**, 628–640 (2011)

[15] Milewski, P.A., Vanden-Broeck, J.-M., Wang, Z.: Steady dark solitary flexural gravity waves. Proc. R. Soc. A **469**(2150), 20120,485 (2013)

[16] MilewskiI, P.A., Vanden-Broeck, J.-M., Wang, Z.: Dynamics of steep two-dimensional gravity–capillary solitary waves. Journal of Fluid Mechanics **664**, 466–477 (2010)

[17] Papageorgiou, D., Vanden-Broeck, J.-M.: Antisymmetric capillary waves in electrified fluid sheets. European Journal of Applied Mathematics **15**(06), 609–623 (2004)

[18] Papageorgiou, D.T., Petropoulos, P.G., Vanden-Broeck, J.-M.: Gravity-capillary waves in fluid layers under normal electric fields. Physical Review E **72**(5), 051,601 (2005)

[19] Papageorgiou, D.T., Vanden-Broeck, J.-M.: Large-amplitude capillary waves in electrified fluid sheets. Journal of Fluid Mechanics **508**, 71–88 (2004)

[20] Papageorgiou, D.T., Vanden-Broeck, J.-M.: Numerical and analytical studies of non-linear gravity–capillary waves in fluid layers under normal electric fields. IMA journal of applied mathematics **72**(6), 832–853 (2007)

[21] Plotnikov, P., Toland, J.F.: Modelling nonlinear hydroelastic waves. Philosophical Transactions of the Royal Society of London A: Mathematical, Physical and Engineering Sciences **369**(1947), 2942–2956 (2011)

[22] Tilley, B., Petropoulos, P., Papageorgiou, D.: Dynamics and rupture of planar electrified liquid sheets. Physics of Fluids **13**(12), 3547–3563 (2001)

[23] Vanden-Broeck, J.-M.: Gravity-capillary free-surface flows. Cambridge University Press (2010)

[24] Vanden-Broeck, J.-M.: On periodic and solitary pure gravity waves in water of infinite depth. Journal of Engineering Mathematics **84**(1), 173–180 (2014)

[25] Vanden-Broeck, J.-M.: New families of pure gravity waves in water of infinite depth. Wave Motion **72**, 133–141 (2017)

[26] Wang, Z.: Modeling nonlinear electrohydrodynamic surface waves over three-dimensional conducting fluids. Proceedings of the Royal Society **473**, 2200 (2017)